

# Oxidized Low-Density Lipoprotein Is Present in Astrocytes Surrounding Cerebral Infarcts and Stimulates Astrocyte Interleukin-6 Secretion

Feng-Shiun Shie,\* M. Diana Neely,<sup>†</sup>  
Izumi Maezawa,\* Hope Wu,<sup>†</sup> Sandy J. Olson,<sup>†</sup>  
Günther Jürgens,<sup>‡</sup> Kathleen S. Montine,\* and  
Thomas J. Montine\*

From the Department of Pathology,\* University of Washington, Seattle, Washington; the Department of Pathology,<sup>†</sup> Vanderbilt University, Nashville, Tennessee; and the Institute of Medical Biochemistry,<sup>‡</sup> Karl-Franzens Universität Graz, Graz, Austria

**Ischemic injury to brain is associated with both disruption of the blood-brain barrier and increased oxidative stress. Given the neurotoxicity associated with exposure to oxidized low-density lipoprotein (oxLDL) *in vitro*, we tested the hypothesis that oxLDL may be present in parenchymal cells of cerebrum after infarction and that oxLDL may influence the pathophysiology of cerebral infarction. Our results showed that the subacute phase of cerebral infarction in patients was characterized by the appearance of oxLDL epitopes in astrocytes, but not neurons or microglia, in the perinecrotic zone. We further demonstrated that minimally oxLDL was most effectively internalized by primary cultures of rat astrocytes, and that exposure to minimal oxLDL stimulated astrocyte interleukin-6 secretion but did not alter nitric oxide production. These results demonstrate for the first time that oxLDL is present in brain parenchyma of patients with ischemic infarction and suggest a potential mechanism by which oxLDL may activate innate immunity and thereby indirectly influence neuronal survival. (*Am J Pathol* 2004, 164:1173–1181)**

Lipoproteins are complex structures that orchestrate lipid trafficking through direct interaction with cell membranes and through receptor-mediated processes with apolipoproteins. Low-density lipoprotein (LDL) and its major apolipoprotein, apoB, are prone to oxidation in circulation and the resultant oxidized (ox)LDL is thought to be a key element in atherogenesis.<sup>1</sup> Increasing evidence shows that oxLDL is internalized by or activates cell-surface receptors on endothelial cells, vascular smooth muscle cells, and monocytes/macrophages, and thereby alters several cellular functions that can culminate in cell death.<sup>2</sup> Indeed, oxLDL is cytotoxic to many cell types in culture primarily through these receptor-dependent pro-

cesses. Importantly, the pathophysiology of oxLDL is much more complicated than simply inducing death in cultured cells; oxLDL also affects leukocyte adhesion, motility of various cell types, growth factor production, and activation of innate immunity.<sup>3</sup>

In our original description of central nervous system (CNS) lipoproteins from patients with Alzheimer's disease (AD), we detected disease-related changes in lipids that are consistent with increased oxidation of CNS lipoproteins compared to age-matched controls.<sup>4</sup> We subsequently demonstrated that minimally oxidized human cerebrospinal fluid lipoproteins are toxic to cultured neurons, establishing that oxidation of lipoproteins normally residing in the CNS is capable of inducing neuron cell death in culture.<sup>5,6</sup> Similarly, others have demonstrated neuronal cytotoxicity from oxLDL. Specifically, oxLDL mediates time- and dose-dependent cytotoxicity to primary cultures of embryonic rodent cerebral and hippocampal neurons but not astrocytes or microglia.<sup>7,8</sup> Unlike experiments with minimally oxidized cerebrospinal fluid lipoproteins, these experiments with oxLDL did not include characterizing the extent of LDL oxidation, a variable known to significantly impact biological activity.

The CNS produces astrocyte-derived lipoproteins that circulate in extracellular fluid of brain and cerebrospinal fluid and are distinctly separated from their plasma counterparts by the blood-brain barrier (BBB).<sup>9</sup> Indeed, although astrocytes can produce lipoproteins with varying densities including some that have densities similar to LDL, multiple laboratories have repeatedly shown that neither apoB mRNA nor protein is present in the developed CNS of several species, including humans, demonstrating the incapacity of CNS cells to produce apoB-containing lipoproteins, such as LDL.<sup>4,10,11</sup> These data question the relevance of oxLDL as an effector of neurodegeneration in AD. In contrast, ischemic injury to brain

---

Supported by the Ellsworth and Nancy Alvord Endowed Chair in Neuro-pathology (to T.J.M.), the National Institutes of Health (grant R01AG16835), and the American Heart Association (grant 0160221B to M.D.N.).

F.-S.S. and M.D.N. contributed equally to this work and should be considered co-first authors.

Accepted for publication December 5, 2003.

Address reprint requests to Thomas J. Montine, M.D., Ph.D., Department of Pathology, University of Washington, Box 359791, Harborview Medical Center, 325 9th Ave., Seattle, WA 98104. E-mail: tmontine@u.washington.edu.

**Table 1.** Patient Information Grouped by Type of Infarct

Type of infarct	Age (years)	Gender	Underlying disease
Acute	48	M	Gastrointestinal hemorrhage
	72	M	Myocardial infarction
	87	F	Myocardial infarction
Subacute	1.5	F	Disseminated intravascular coagulation
	25	F	Systemic lupus erythematosus
	44	F	Pancytopenia
	59	M	Acute leukemia
	65	M	Metastatic carcinoma
	66	F	Hypertension/pneumonia
Remote	42	F	Systemic lupus erythematosus
	61	M	Lymphoma
	63	M	Cirrhosis

clearly is associated with disruption of the BBB,<sup>12</sup> raising the possibility of exposing the CNS to plasma lipoproteins. In combination with disruption of the BBB, numerous studies have associated cerebral infarction with increased oxidative stress derived from glia, neurons, and endothelium.<sup>13</sup> Given that CNS infarction is associated with BBB disruption and increased oxidative stress, we tested the hypothesis that oxLDL, a known neurotoxin in cell culture, would be incorporated into cells in the vicinity of ischemic damage and that this interaction may alter the pathophysiology of infarct progression.

## Materials and Methods

### Patient Material

Cases were selected by timing of cerebral cortical infarct relative to death as acute (less than 1 day), subacute (between 1 day and 2 weeks), and remote (greater than 1 month); otherwise cases were chosen randomly from autopsy files. Characteristics of the patients are given in Table 1. All tissue was fixed in formalin for 10 to 14 days, dissected, and blocks embedded in paraffin. Histopathological grading of infarcts was performed using established criteria with hematoxylin and eosin-stained tissue sections.<sup>14</sup> Also analyzed were sections of hippocampus and temporal cortex from five patients with AD as classified by National Institute on Aging-Reagan Institute criteria.<sup>15</sup>

### Immunohistochemistry

Immunohistochemistry for oxLDL epitopes was performed with two different widely used antibodies. The first was rabbit polyclonal anti-hypochlorite oxLDL antibody (AB3232) from Chemicon (Temecula, CA) that is highly specific for immunohistochemical analysis of oxLDL epitopes. The second antibody was a mouse monoclonal anti-Cu<sup>2+</sup>-oxLDL antibody (OB/04) with demonstrated high specificity for oxLDL that also has been used for immunohistochemical analysis of atherosclerotic lesions.<sup>16</sup> Both antibodies gave identical results in our studies. Other primary antibodies included anti-glial fibril-

lary acidic protein, anti-CD68, and anti-4-hydroxy-2-nonenal (HNE) protein adduct antibodies used exactly as previously described, as was the protocol for single- and double-antigen detection.<sup>17,18</sup>

### Dil Labeling

Human LDL was purchased from Calbiochem (La Jolla, CA) and 1,1'-dioctadecyl-3,3',3' tetramethylindocarbocyanine perchlorate (Dil) was purchased from Molecular Probes (Eugene, OR). To label LDL with Dil, 1 mg of LDL and 100  $\mu$ l of 3-mg Dil/ml dimethyl sulfoxide were brought up to 1 ml in phosphate-buffered saline (PBS), incubated at 37°C for 16 hours, passed through a 0.22- $\mu$ m filter, and desalted using a PD-10 column (Amersham, Piscataway, NJ).

### Oxidation

AAPH (2,2'-azobis(2-amidinopropane) dihydrochloride) (Sigma, St. Louis, MO) was incubated at 37°C with Dil-labeled LDL (Dil-LDL) under the following three conditions: 1 mmol/L AAPH for 5 hours (Dil-oxLDL-L), 1 mmol/L AAPH for 16 hours (Dil-oxLDL-M), or 10 mmol/L AAPH for 16 hours (Dil-oxLDL-H). After oxidation, each Dil-oxLDL preparation was subjected to extensive dialysis against five changes of PBS for 24 hours at 4°C followed by centrifugation using Centricon YM-100 (Millipore, Bedford, MA) and filter sterilization. To ensure that AAPH oxidation did not affect Dil fluorescence, fluorescence was compared between Dil-LDL and the three different Dil-oxLDL preparations. Fluorescence intensity was quantified using the procedure of Teupser and colleagues<sup>19</sup> with minor modifications. Samples were dissolved in lysis buffer containing 0.1% sodium dodecyl sulfate and 0.1% NaOH for 1 hour. Fluorescence was measured in 2- $\mu$ l duplicates of lysate using a fluorescence plate reader (Spectra Max 250; Molecular Devices, Sunnyvale, CA) with excitation and emission wavelengths at 520 and 580 nm, respectively. Data were corrected for autofluorescence of the lysis buffer and normalized for protein concentration. Dil fluorescence was not significantly different among all groups, indicating that AAPH oxidation did not affect the intensity of Dil fluorescence.

### $\alpha$ -Tocopherol Analysis

$\alpha$ -Tocopherol levels were quantified by reverse-phase, high-performance liquid chromatography. Five  $\mu$ l of internal standard, 1 mmol/L  $\alpha$ -tocopherol acetate, was added to 300  $\mu$ l of Dil-LDL or Dil-oxLDL sample. Three hundred  $\mu$ l of methanol was then added and the mixture vortexed for 30 seconds. Nine hundred  $\mu$ l of high-performance liquid chromatography grade hexane was added, and the mixture was vortexed vigorously for 2 minutes and centrifuged briefly to separate phases. The organic phase was transferred to another tube and evaporated under a stream of nitrogen in a 37°C water bath. The residue was suspended in 150  $\mu$ l of ethanol, and 40  $\mu$ l of

this was injected onto the chromatographic column. The high-performance liquid chromatography system consisted of a Shimadzu (Columbia, MD) LC-10ADvp pump, a C18 reverse-phase column, and a Shimadzu RF-10AxI fluorescence detector. Samples were eluted with 100% methanol (mobile phase) at a flow rate of 1 ml/min. The fluorescence detector was set to monitor wavelengths of emission at 292 nm and excitation at 335 nm.  $\alpha$ -Tocopherol levels were determined by comparing the area of each sample to that of the internal standard.

### Quantification of $F_2$ -Isoprostanes and Isofurans

$F_2$ -isoprostanes ( $F_2$ -IsoPs) and isofurans (IsoFs) were quantified by stable isotope dilution gas chromatography/negative ion chemical ionization/mass spectrometry (GC/NICI/MS) as previously described.<sup>20,21</sup> Samples were homogenized using a Brinkmann polytron motorized tissue grinder, and lipids were extracted using the Folch method (chloroform:methanol 2:1 v/v) supplemented with 0.005% (w/v) butylated hydroxytoluene to prevent auto-oxidation. After evaporation to dryness under nitrogen, lipids were hydrolyzed with 15% (w/v) potassium hydroxide to release esterified  $F_2$ -IsoPs and IsoFs, and the internal standard [ $^2H_4$ ]15- $F_{2t}$ -IsoP added to the samples. These products were then extracted using C18 and silica Sep-Paks, derivatized to pentafluorobenzyl esters, further purified by thin-layer chromatography, and derivatized to trimethylsilyl esters. These derivatives were analyzed by selected ion monitoring GC/NICI/MS of m/z 569 for  $F_2$ -IsoPs, m/z 585 for IsoFs, and m/z 573 for the internal standard [ $^2H_4$ ]15- $F_{2t}$ -IsoP.

### Apolipoprotein B (ApoB) Western Blot Analysis

Dil-LDL and Dil-oxLDLs were diluted with 2 $\times$  Laemmli buffer and boiled for 10 minutes. The samples were subjected to 5% Tris-HCl sodium dodecyl sulfate-polyacrylamide gel electrophoresis, transfer, and Western blotting for analysis of protein degradation. Rabbit polyclonal antibody against apoB (Bioscience Resource Project, Saco, ME) was used at a dilution of 1:1000. Horseradish peroxidase-conjugated goat anti-rabbit antibody (Amersham) was used as secondary antibody. Immunoreactivity was visualized with enhanced chemiluminescence (Amersham).

### Rat Astrocyte Primary Cultures

Rat primary astrocytes were derived from cerebral cortices of neonatal (postnatal day 3) Sprague-Dawley rats (Charles River, Wilmington, MA). The procedure is adopted from Ye and Sontheimer<sup>22</sup> with slight modifications. Tissues were dissected in ice-cold Dulbecco's modified Eagle's medium (Life Technologies, Inc., Carlsbad, CA). Enzyme solution containing Dulbecco's modified Eagle's medium, 0.5 mmol/L ethylenediaminetetraacetic acid (Sigma), 0.2 mg/ml of L-cysteine (Sigma), 30 U/ml papain (Worthington, Lakewood, NJ), and 200  $\mu$ g/ml of Dnase I (Worthington) was used. Cells were seeded on 0.001% poly-L-ornithine (Sigma)-coated T-175

plates (Sarstedt, Newton, NC) with Dulbecco's modified Eagle's medium containing 10% fetal bovine serum (Hyclone, Logan, UT) and penicillin/streptomycin (Sigma). After 14 to 18 days in culture, astrocytes were trypsinized and plated onto chambered cover glasses (Lab-Tek, Naperville, IL) and incubated for 48 hours before treatments.

### Exposure to Dil-LDL or Dil-oxLDL

Dil-LDL or Dil-oxLDL was applied to all astrocyte cultures at 20  $\mu$ g of protein/ml of culture medium without fetal bovine serum for 24 hours. Four separate experiments for each treatment were performed. After treatment, culture medium was collected and stored at  $-20^\circ\text{C}$  for interleukin (IL)-6 and nitric oxide assays, while cells were washed with PBS and fixed with 4% paraformaldehyde in PBS for cell count, Dil uptake quantification, and immunocytochemistry. To evaluate cell death, cell number in all groups was determined by counting nuclei counterstained with 4',6-diamidino-2-phenylindole-containing mounting medium (Molecular Probes). Triplicate images from each experimental group were randomly taken using Nikon TE200 fluorescent inverted microscope (Meridian Instrument, Kent, WA). Images were printed and nuclei counted manually. Cell count was not significantly different among all groups.

### Quantification of Dil-LDL Uptake

Three images of paraformaldehyde-fixed culture were randomly taken with a confocal microscope and two photon imaging system. Images were collected at a wavelength of  $580 \pm 10$  nm using a krypton laser, and the imaging system was programmed at identical settings using a  $\times 25$  objective. Images were edited and subjected to analysis using MetaMorph imaging software (Universal Imaging Corporation, Downingtown, PA). Standard competition experiments using Dil-LDL plus a 10-fold higher concentration of unlabeled LDL were performed to confirm that Dil uptake was not because of free Dil, and indeed excess LDL inhibited Dil uptake  $\sim 95\%$ . These experiments were limited to a 2-hour incubation because longer incubation of astrocytes with this high concentration of LDL (200  $\mu$ g protein/ml) was cytotoxic.

### Co-Localization of oxLDL Epitope, Dil-LDL, and Cholesterol

Paraformaldehyde-fixed astrocyte cultures were washed with PBS and incubated with anti-oxLDL antibody AB3232 (described above) at a dilution of 1:100 followed by secondary antibody conjugated to Alexa Fluor 633 (Molecular Probes). The antibody solution also contained filipin (Sigma) at 100  $\mu$ g/ml for staining free cholesterol. Images were taken using confocal microscopy as described above by collecting fluorescent emissions at  $580 \pm 10$ ,  $500 \pm 10$ , and  $649 \pm 10$  nm from Dil, filipin, and Alexa Fluor 633, respectively.

## IL-6 Assay

Secreted IL-6 levels were determined using a rat IL-6 enzyme-linked immunosorbent assay kit (Biosource Int., Camarillo, CA). Quantification was performed using a microplate reader according to the manufacturer's instructions. As a positive control for IL-6 secretion, lipopolysaccharide (LPS, Sigma) was added to astrocytes at 100 ng/ml for 24 hours and medium collected as described above. Competition experiments with excess unlabeled LDL could not be performed because high concentrations of LDL are cytotoxic to astrocytes after prolonged (in this case 24 hours) incubation, as explained above for quantification of Dil uptake.

## Nitric Oxide Assay

Medium concentrations of nitrate and nitrite were determined using a nitric oxide assay kit (Oxis Int., Portland, OR). Briefly, nitrate is first converted to nitrite, and then total nitrite is measured as an indicator of nitric oxide production.

## Statistical Analysis

Data were analyzed using GraphPad Prism (San Diego, CA) software. Analysis of variance was used to test significance between groups. Bonferroni multiple comparisons were used for post hoc tests.  $\alpha$  was set at 0.05.

## Results

To test the hypothesis that oxLDL is incorporated into cells in the vicinity of ischemic damage we undertook immunohistochemical analyses of oxLDL epitopes in autopsy samples of cerebral infarcts from 12 patients (Table 1). Age of infarct was classified as acute (up to 1 day old), subacute (more than 1 day and less than 2 weeks old), or remote (longer than 1 month old) using clinical history and standard histopathological criteria.<sup>14</sup> Acute infarcts showed minimal structural alterations other than tissue edema and occasional hypereosinophilic neurons. Subacute infarcts all showed a necrotic core of partially liquefied tissue with dense macrophage infiltrate surrounded by a perinecrotic zone of partial neuron necrosis and markedly reactive glia. Remote infarcts showed a partially to fully cavitated lesion surrounded by a rim of tissue primarily depleted of neurons and containing chronic reactive astrocytes. In all cases, histopathological timing of the infarct corresponded to clinical history of stroke. Tissue sections from cerebrum uninvolved by infarct were histologically normal.

Immunohistochemical evaluation of cerebral infarct tissue sections for oxLDL epitopes using anti-oxLDL antibody AB3232 showed distinct differences among cell types and infarct age. Tissue sections of cerebrum not involved by infarct did not show immunoreactivity. Acute ischemic damage also typically did not yield immunoreactivity, although a few scattered immunoreactive astrocytes were identified. In subacute ischemia, intensely

oxLDL-immunoreactive cells with the morphological features of reactive astrocytes formed a rim surrounding the necrotic core (Figure 1A). Higher power magnification of oxLDL-immunoreactive cells in the perinecrotic zone details their reactive astrocyte morphology (Figure 1B). Another high-power image showing oxLDL-immunoreactive cells in the perinecrotic zone were also immunoreactive for glial fibrillary acidic protein (Figure 1C). We did not observe cells with the morphological features of microglia that were immunoreactive for oxLDL, nor did oxLDL immunoreactivity co-localize with CD68 immunoreactivity (not shown). Although there was substantial neuron loss in the perinecrotic zone of subacute infarcts, those neurons remaining were not immunoreactive for oxLDL epitopes (Figure 1A). The oxLDL immunoreactivity was restricted to the perinecrotic zone and did not extend out to histologically normal-appearing cerebrum in the same tissue section. Within this zone, the walls of small arterioles, often with hyalinization, also showed immunoreactivity for oxLDL epitopes (Figure 1D). There were no apparent differences with respect to differing ages of patients or underlying disease. No oxLDL immunoreactivity was observed in any section of remote infarct. Immunohistochemical results using anti-oxLDL antibody OB/04 were identical. Thus, immunoreactivity for oxLDL epitopes was localized to reactive astrocytes and arteriole walls in the perinecrotic zone of subacute infarcts.

Because the zone where we observed increased oxLDL immunoreactivity in astrocytes has likely been exposed to high level of oxidative stress, it was possible that the immunoreactivity we observed was the result of cross-reaction of oxLDL antibody with other oxidized protein epitopes. To verify that the oxLDL antibodies were not recognizing oxidized protein epitopes in general, we tested our antibodies on tissue known to be abundant in products of oxidative damage. Previously we and others have used a variety of antibodies to oxidized protein epitopes and protein carbonyls in AD brain and have localized immunoreactivity primarily to pyramidal neuron soma and neuropil in diseased regions of cerebrum.<sup>23</sup> In our case, we have used antibodies that specifically recognize HNE-protein adducts.<sup>4,18</sup> This time we compared anti-HNE and anti-oxLDL immunoreactivity in tissue sections from diseased regions of brain from five patients with AD; these tissue sections were taken from the medial temporal lobe including hippocampus and entorhinal cortex, the last showing the most extensive astrogliosis in AD brain. As expected, there was extensive HNE immunoreactivity present (Figure 2A); however, there was no immunoreactivity with either oxLDL antibody AB3232 (Figure 2B) or OB/04 (not shown) in sections from any AD patient. Conversely, we performed immunohistochemistry using anti-HNE protein adduct antibody on tissue sections from the subacute infarcts studied above. In agreement with what others have described for HNE immunoreactivity after ischemia to cerebrum,<sup>24</sup> we observed immunoreactivity localized to cytoplasm of the remaining neurons and neuropil in the perinecrotic zone, but not astrocytes (not shown). Taken together, these results confirmed that the oxLDL antibodies used here



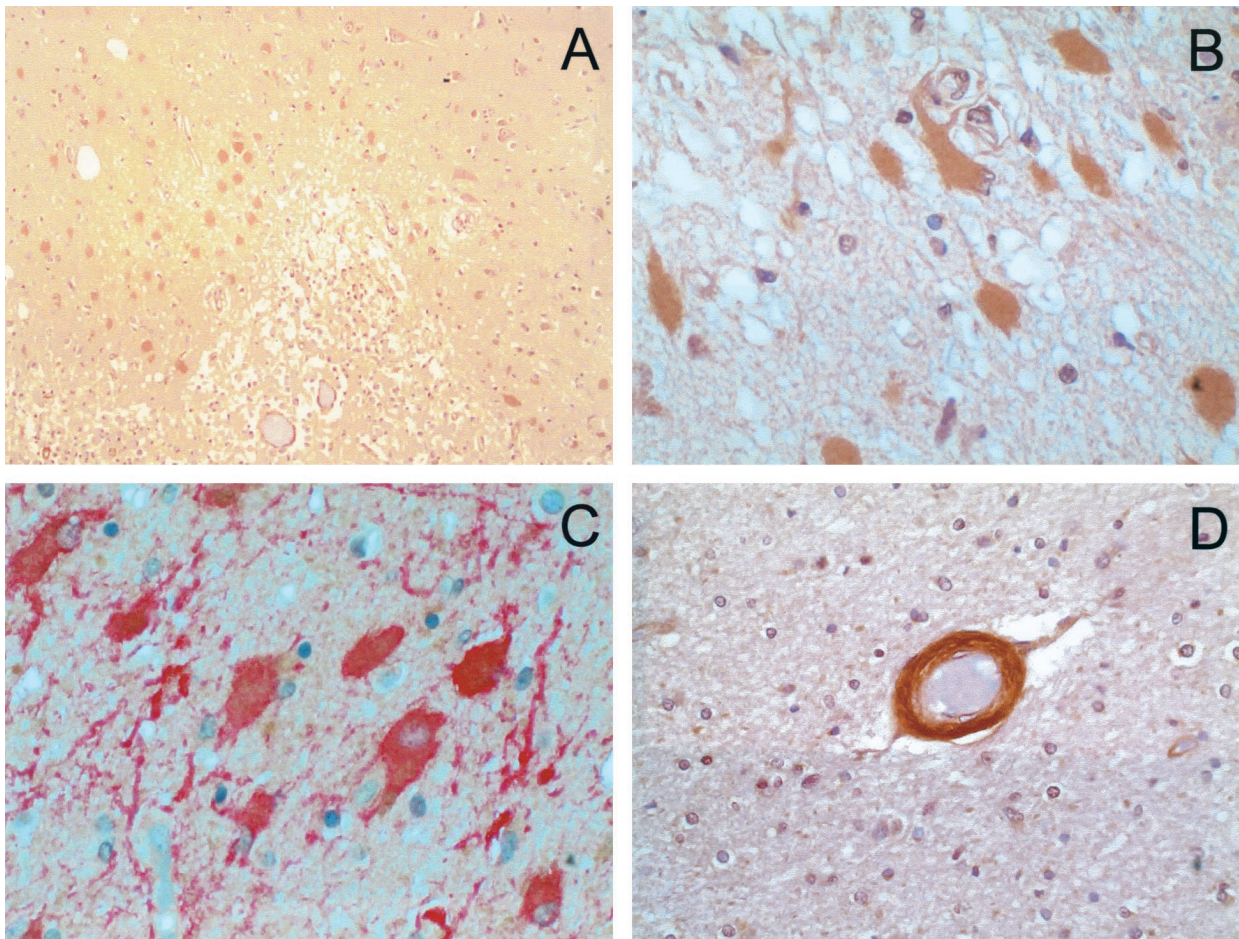


**Figure 1.** Immunohistochemical detection of oxLDL epitopes in subacute cerebral infarcts using anti-oxLDL antibody AB3232 and hematoxylin counter stain. **A:** Necrotic core (**bottom**) is surrounded by oxLDL immunoreactive cells (brown chromogen). **B:** Higher magnification of **A** showing oxLDL immunoreactivity in soma and processes of reactive astrocytes. **C:** Reactive astrocytes in the perinecrotic zone show both oxLDL epitopes (brown chromogen) and glial fibrillary acidic protein (red chromogen). **D:** OxLDL (brown chromogen) immunoreactivity with thickened arteriole wall. Original magnifications:  $\times 100$  (**A**);  $\times 600$  (**B**);  $\times 200$  (**D**).

recognized specific epitopes and not oxidized protein in general.

Because our immunohistochemical results indicated that oxLDL epitopes were incorporated into astrocytes in the perinecrotic zone of subacute infarcts, we next undertook a series of experiments with oxLDL and primary cultures of astrocytes to confirm *in vitro* that oxLDL was internalized by astrocytes and to determine whether this had pathophysiological significance. The first step in these experiments was to prepare and characterize LDL oxidized to different extents. We used a standard method

of AAPH-mediated oxidation to yield controlled, low-level free radical flux.<sup>25</sup> LDL was first labeled with the lipophilic fluorescent dye Dil (Dil-LDL) and then oxidized under three different conditions: 1 mmol/L AAPH for 5 hours (Dil-oxLDL-L), 1 mmol/L for 16 hours (Dil-oxLDL-M), and 10 mmol/L AAPH for 16 hours (Dil-oxLDL-H) to achieve different levels of oxidation. Dil fluorescence as detected by fluorometry was not altered by oxidation (not shown). To characterize the extent of oxidative damage to the three preparations, we quantified  $\alpha$ -tocopherol as a measure of antioxidant capacity,  $F_2$ -IsoPs and IsoFs as mark-

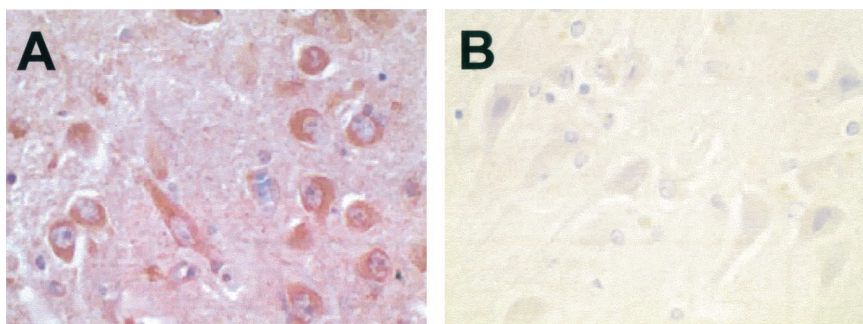


**Figure 2.** Immunohistochemical detection of anti-HNE protein adducts (**A**) and oxLDL epitopes (**B**) in hippocampal sections from a patient with AD. AB3232 was used for oxLDL. Immunoreactivity was visualized with diaminobenzidine as chromogen substrate (brown) on sections counterstained with hematoxylin. Original magnifications,  $\times 600$ .

**Table 2.** Biochemical Changes in Dil-oxLDL with Low (-L), Medium (-M), or High (-H) Oxidation

Particle	$\alpha$ -Tocopherol (% control)	F <sub>2</sub> -IsoPs (ng/mg protein)	IsoFs (ng/mg protein)
Dil-LDL	100 ± 3.8	11 ± 3	16 ± 6
Dil-oxLDL-L	62.8 ± 0.9*	49 ± 3*	80 ± 8*
Dil-oxLDL-M	73.7 ± 0.7*	66 ± 6*	109 ± 17*
Dil-ox-LDL-H	23.8 ± 1.8*	27 ± 4*	102 ± 16*

Analysis of variance for all three measures was statistically significant ( $P < 0.05$ ).

\*,  $P < 0.05$  compared to Dil-LDL using Bonferroni-corrected repeated pair comparisons.

ers of lipid peroxidation, and altered apoB immunoreactivity as a marker of protein damage (Table 2 and Figure 3). F<sub>2</sub>-IsoPs are well-known quantitative biomarkers of lipid peroxidation derived from arachidonic acid. IsoFs are recently described products of the same pathway whose formation is favored over IsoPs under conditions of increased oxygen tension, such as cell culture experiments and *ex vivo* oxidation, as occurred in the experiments described here.<sup>21</sup> LDL oxidation displayed the expected sequence of well-described changes.<sup>26</sup> Dil-oxLDL was oxidized under three different conditions that yielded increasingly damaged LDL, as evidenced by consumption of  $\alpha$ -tocopherol, increase in F<sub>2</sub>-IsoPs and IsoFs, and degradation of apoB immunoreactivity. It is noteworthy that F<sub>2</sub>-IsoPs were lower in Dil-oxLDL-H compared to Dil-oxLDL-M; decreasing F<sub>2</sub>-IsoPs in extensively oxidized LDL has been observed previously<sup>27</sup> and likely results from further oxidation of IsoPs under these extreme conditions.

We incubated cell cultures of primary astrocytes with one of these oxidized Dil-LDL preparations or Dil-LDL for 24 hours. Cell counts were performed to evaluate cell death during treatments. Results showed that there was no significant difference in cell number among groups, in accord with results of others showing lack of astrocyte cytotoxicity when exposed to oxLDL.<sup>7,8</sup> We then measured Dil-oxLDL uptake by astrocytes using confocal microscopy to determine the amount of Dil incorporated

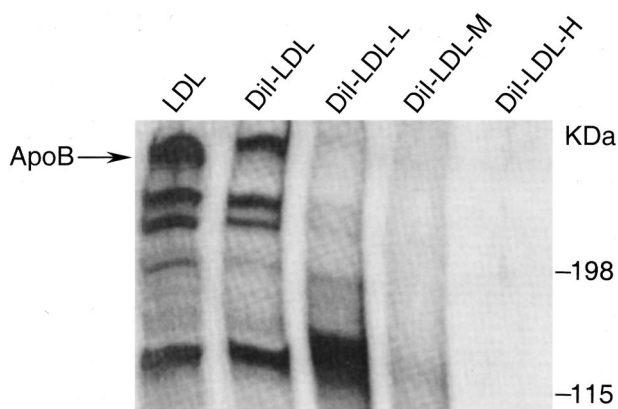


**Figure 3.** Representative Western blot of apoB from unlabeled LDL, Dil-LDL, and Dil-oxLDL with low (-L), medium (-M), or high (-H) oxidation. Unlabeled LDL and Dil-LDL had similar apoB immunoreactivity. Dil-oxLDL-L had reduced apoB antigenicity and increased low-molecular weight species consistent with protein degradation, whereas apoB immunoreactivity was greatly diminished in Dil-oxLDL-M and completely absent in Dil-oxLDL-H.

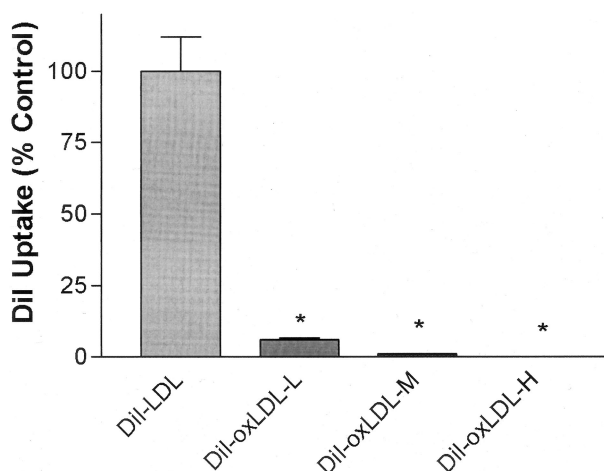


**Figure 4.** Dil-oxLDL uptake by astrocytes after 24-hour exposure was measured by comparing the intensity of intracellular Dil fluorescence to that of astrocytes exposed to Dil-LDL using confocal microscopy as described in Materials and Methods. Data are expressed as percent control of Dil-LDL and are mean ± SEM for three separate experiments. Analysis of variance for all four groups was statistically significant ( $P < 0.0001$ ). \*,  $P < 0.001$  for Bonferroni-corrected repeated pair comparisons with Dil-LDL.

into cells (Figure 4) and compared it to Dil-LDL uptake (control). Dil uptake in cells exposed to Dil oxLDL-L was reduced to  $5.7 \pm 0.7\%$  of control, while Dil-oxLDL-M uptake was reduced to  $0.9 \pm 0.1\%$  of control, and uptake of Dil-oxLDL-H was undetectable.

To confirm that the Dil uptake we observed with Dil-oxLDL-L represented oxLDL uptake and not a residual nonoxidized component of the Dil-oxLDL-L preparation, we performed immunocytochemical analysis on astrocytes exposed to Dil-oxLDL-L or Dil-LDL using one of the antibodies (AB3232) from the human tissue studies described above. Analysis by confocal microscopy showed that the oxLDL epitope was detected within astrocytes exposed to Dil-oxLDL-L (Figure 5A), and that this epitope co-localized with Dil label and the majority of filipin stain for cholesterol, consistent with the uptake of cholesterol-rich Dil-oxLDL-L by astrocytes. In contrast, the small amount of immunoreactivity to the oxLDL epitope we observed in astrocytes exposed to Dil-LDL was not greater than background levels (Figure 5B).

One effect of oxLDL thought to be important to atherogenesis is its ability to modify the secretion of specific cytokines such as IL-6 by monocytes and macrophages.<sup>28</sup> In addition, astrocytes are the major source of IL-6 in brain and astrocyte-secreted IL-6 has been proposed to influence neuronal survival during ischemic infarction.<sup>29</sup> Therefore we next determined whether exposure to Dil-oxLDL stimulated astrocyte IL-6 secretion into cell culture medium (Figure 6). Untreated astrocytes did not secrete any detectable IL-6, whereas exposure to LPS as a positive control markedly increased IL-6 secretion ( $P < 0.001$ ). Exposure to Dil-oxLDL-L stimulated astrocyte IL-6 secretion to the same extent as LPS, whereas exposure to Dil-oxLDL-M or Dil-oxLDL-H led to little or no detectable IL-6 secretion, respectively. Interpreting the progressively smaller increase in IL-6 secretion with increasing oxidation of Dil-LDL in light of the Dil-uptake data (Figure 4) strongly suggests that expo-



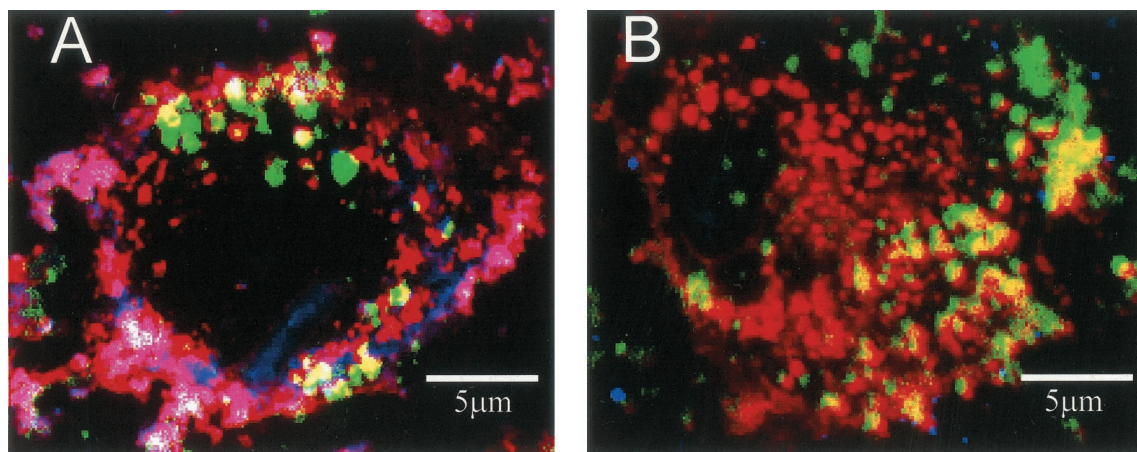


**Figure 5.** Co-localization of oxLDL epitope, DiI label, and cholesterol in astrocytes exposed to DiI-oxLDL-L (**A**) or DiI-LDL (**B**) for 24 hours. Antibody AB3232 (blue) and filipin (green) were used to localize oxLDL epitope and cholesterol, respectively. DiI in these images is red. Purple/pink depicts co-localization of DiI and oxLDL. White depicts co-localization of all three molecules. **A:** OxLDL immunoreactivity co-localized with DiI and the majority of filipin staining in astrocytes exposed to DiI-oxLDL-L. **B:** DiI predominantly co-localized with filipin in cells exposed to DiI-LDL. There was also a small amount of immunoreactivity for oxLDL; however, this was not greater than background levels.

sure to oxLDL itself was not sufficient to cause IL-6 production, but rather that some oxLDL cellular uptake was required to stimulate IL-6 secretion. Interestingly, DiI-LDL stimulated IL-6 secretion over untreated controls to levels approximately one-third that of DiI-oxLDL-L.

Because of the central role of increased activity of nitric oxide synthases in the pathogenesis of cerebral ischemia, we also determined astrocyte nitrate and nitrite (assayed together) concentrations as an indicator of nitric oxide production in the same medium as that used for the IL-6 assay. Nitrate/nitrite levels in untreated controls were  $2.51 \pm 0.10 \mu\text{mol/L}$ . Levels after LPS, DiI-LDL, or DiI-oxLDL-L exposure were  $3.03 \pm 0.14$ ,  $2.85 \pm 0.14$ , or  $2.57 \pm 0.14 \mu\text{mol/L}$ , respectively ( $n = 4$  in all experiments). Only LPS-treated cultures were significantly different from controls ( $P < 0.05$ ).

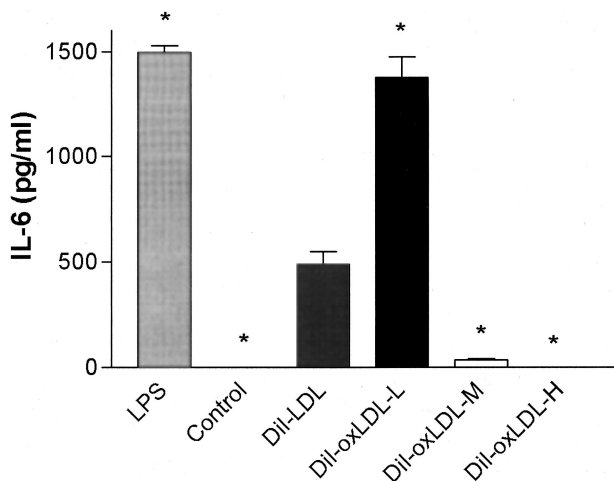


**Figure 6.** IL-6 concentrations were determined in culture media after a 24-hour incubation of astrocytes with LPS, DiI-LDL, or DiI-oxLDL with low (-L), medium (-M), or high (-H) oxidation. Untreated astrocytes had no detectable IL-6. Data are presented as mean  $\pm$  SEM for  $n \geq 3$  separate experiments. Analysis of variance was statistically significant for the six groups ( $P < 0.0001$ ). \*,  $P < 0.001$  for Bonferroni-corrected repeated pair comparisons.

### Discussion

We tested the hypothesis that oxLDL is generated during cerebral infarction and thus may contribute to its pathogenesis. Our results from two widely used and well-characterized antibodies that specifically recognize oxLDL epitopes showed immunoreactivity localized to soma and processes of reactive astrocytes and arteriole walls in the perinecrotic zone of subacute infarcts. Importantly, no immunoreactivity was observed with neurons or microglia. Subsequent experiments showed that primary cultures of astrocytes internalized oxLDL-L and this was associated with increased secretion of IL-6, but no change in nitric oxide production.

Immunoreactivity for oxLDL epitopes was minimal in acute infarcts, abundant in the perinecrotic zone of subacute infarcts, and not detectable in remote infarcts. The mechanistic basis for this sequence is not clear but one possibility is that it may be related to the confluence of two processes: disruption of the BBB and increased free radical generation. BBB disruption after infarction is a complex process but its progression can be approximated by vasogenic edema, which is caused by increased permeability of the BBB. The time course of vasogenic edema after cerebral infarction is well described in patients and experimental animals and is similar to what we observed with oxLDL immunoreactivity: minimal effect in the first hours after infarction that then progressively increases throughout the next several days and returns to normal throughout a few weeks.<sup>30</sup> Although the time course of free radical generation is not as well characterized in patients with cerebral infarction, it has been investigated in detail in rodent models of cerebral ischemia in which there is a delay of several hours after infarction followed by significantly increased free radical generation that then peaks  $\sim 2$  days after infarction.<sup>31</sup> Another possibility is that, at least for those patients with underlying diseases that suggest increased levels of circulating oxLDL, ischemic injury may have

permitted entry of circulating oxLDL into cerebral arterioles and CNS rather than oxLDL being formed locally. The lack of oxLDL epitopes in remote infarcts may be because of reversal of both BBB disruption and increased free radical generation, coupled with proteolytic degradation of oxLDL epitopes previously incorporated into astrocytes.

Although others have shown that oxLDL can be toxic to neurons in culture,<sup>7,8</sup> we did not observe any oxLDL immunoreactivity in neurons. However, drawing conclusions about the role of oxLDL in neuron death from our study of postmortem tissue is limited because large numbers of neurons die within minutes of cerebral infarction. Although their remains are detectable histologically for days, evidence of neuronal oxLDL immunoreactivity may not remain. Nevertheless, there were some surviving neurons, albeit greatly reduced in number, in the perinecrotic zone; although none of these were immunoreactive for oxLDL epitopes, they were immunoreactive for HNE, indicating that oxidative damage to neuronal proteins occurred. If these neurons were characteristic of those that died, then our results call into question the relevance of *in vitro* studies demonstrating direct neurotoxicity from oxLDL. If these surviving neurons were different from those that died, perhaps in their inability to take up oxLDL, then our results cannot be extended to evaluate the relevance of previous cell culture experiments. Thus, although our results from postmortem studies cannot discern whether or not oxLDL directly contributed to neuron death, they do indicate that the surviving neurons, despite evidence of oxidative damage from HNE, did not contain oxLDL epitopes.

In contrast to a potential direct effect of oxLDL on neuronal survival, our results indicated that oxLDL was internalized by astrocytes, both in human brain and in rat primary cultures. Therefore, we assayed IL-6 and nitric oxide levels in culture medium as indicators of astrocyte activation because IL-6 is the major cytokine produced by astrocytes and activation of nitric oxide synthases is thought to be central to the pathogenesis of cerebral ischemia.<sup>29</sup> Our results showed that of the two, only IL-6 secretion was modified by oxLDL. The role of IL-6 in activation of innate immunity in brain has been described in a number of pathological conditions, including ischemic stroke. Increased cerebrospinal fluid IL-6 levels are significantly correlated with infarct size and functional recovery in patients.<sup>32–34</sup> Unfortunately, evaluation of changes in IL-6 in postmortem tissue from patients with stroke is confounded by the acute transient nature of IL-6 elevation; rodent models have shown that IL-6 mRNA in ischemic cerebral cortex is first significantly increased at 3 hours, peaks at 12 hours, and returns to baseline at ~24 hours after infarction.<sup>35</sup> Despite these associations between IL-6 production and cerebral ischemia, mice lacking the gene for IL-6 do not have significantly different infarct size or neurological function 24 hours after focal cerebral ischemia.<sup>36</sup> One possible explanation for this apparent paradox is that increased IL-6 production may contribute to pathogenic events that occur later. Alternatively, IL-6 may be a marker of activated innate

immunity in patients but may not directly contribute to infarct pathogenesis.

Although our cell culture results clearly cannot resolve the precise role of IL-6 in infarct progression *in vivo*, they are important in the interpretation of our oxLDL uptake results. First, they indicate that the effect of ox-LDL on IL-6 secretion derives from oxLDL uptake; indeed, there was a striking correlation between the extent of uptake of oxLDL and the magnitude of IL-6 secretion among the three different preparations of oxLDL. In contrast, although LDL-exposed astrocytes took up almost 20 times more Dil than those exposed to oxLDL-L, they secreted only ~30% as much IL-6 as those exposed to oxLDL-L, similar to what others have observed in mesangial cells.<sup>37</sup> This ~60-fold difference in stimulated IL-6 secretion per amount of LDL internalized suggests that LDL itself does not stimulate IL-6 production; rather a component of the LDL that has undergone low-level oxidation during collection, Dil labeling, and incubation with cells in culture may be responsible for this effect. This possibility is in agreement with the findings of others who have shown that very low levels of oxLDL exist in blood and that further low-level oxidation occurs during its preparation *ex vivo*.<sup>3</sup> Taken together, it seems likely that the IL-6 secretion we observed in response to LDL may be caused by very low levels of oxLDL. Presumably this very low-level oxidation was below the limit of detection for our immunocytochemical technique, eg, Figure 5B.

In summary, our results showed that cerebral infarction in patients was characterized by the transient appearance of oxLDL epitopes in astrocytes in the perinecrotic zone during the subacute phase. We propose that this results from the confluence of disruption of the BBB and the pro-oxidative environment during cerebral infarction. We next demonstrated that oxLDL can indeed be internalized by astrocytes in culture, albeit to a lesser degree than LDL. In our system, minimal oxLDL was taken up most efficiently, resulting in increased IL-6 secretion by astrocytes without stimulating nitric oxide production. These results demonstrated for the first time that oxidized plasma lipoproteins were present in brain parenchyma of patients with cerebral infarction and suggest an indirect mechanism whereby oxLDL may activate innate immunity and thereby influence neuronal survival.

## References

1. Boullier A, Bird D, Chang M, Dennis E, Friedman P, Gillotte-Taylor K, Horkko S, Palinski W, Quehenberger O, Shaw P, Steinberg D, Terpstra V, Witztum J: Scavenger receptors, oxidized LDL, and atherosclerosis. *Ann NY Acad Sci* 2001, 947:214–222
2. Salvayre R, Auge N, Benoist H, Negre-Salvayre A: Oxidized low-density lipoprotein-induced apoptosis. *Biochim Biophys Acta* 2002, 1585:213–221
3. Horkko S, Binder CJ, Shaw PX, Chang MK, Silverman G, Palinski W, Witztum JL: Immunological responses to oxidized LDL. *Free Radic Biol Med* 2000, 28:1771–1779
4. Montine TJ, Montine KS, Swift LL: Central nervous system lipoproteins in Alzheimer's disease. *Am J Pathol* 1997, 151:1571–1575
5. Bassett CN, Neely MD, Sidell KR, Markesbery WR, Swift LL, Montine TJ: CSF lipoproteins are more vulnerable to oxidation in Alzheimer's disease and are neurotoxic when oxidized *ex vivo*. *Lipids* 1999, 34:1273–1280



6. Neely MD, Swift LL, Montine T: Human, but not bovine, oxidized cerebral spinal fluid lipoproteins disrupt neuronal microtubules. *Lipids* 2000, 35:1249–1257
7. Sugawa M, Ikeda S, Kushima Y, Takashima Y, Cynshi O: Oxidized low density lipoprotein caused CNS neuron cell death. *Brain Res* 1997, 761:165–172
8. Keller JN, Hanni KB, Markesbery WR: Oxidized low-density lipoprotein induces neuronal death. *J Neurochem* 1999, 72:2601–2609
9. Bassett CN, Montine KS, Neely MD, Swift LL, Montine TJ: Cerebrospinal fluid lipoproteins in Alzheimer's disease. *Microsc Res Tech* 2000, 50:282–286
10. Pitas RE, Boyles JK, Lee SH, Hui D, Weisgraber KH: Lipoproteins and their receptors in the central nervous system. *J Biol Chem* 1987, 262:14352–14360
11. Roheim PS, Carey M, Forte T, Vega GL: Apolipoproteins in human cerebrospinal fluid. *Proc Natl Acad Sci USA* 1979, 76:4646–4649
12. del Zoppo GJ, Hallenbeck JM: Advances in the vascular pathophysiology of ischemic stroke. *Thromb Res* 2000, 98:73–81
13. Chan PH: Reactive oxygen radicals in signaling and damage in the ischemic brain. *J Cereb Blood Flow Metab* 2001, 21:2–14
14. Montine TJ, Hulette CM: Pathology of ischemic cerebrovascular disease. *Neurosurgery*. Edited by RR Wilkins, SS Rengachary. New York, McGraw-Hill, 1995, pp 2045–2051
15. Hyman BT, Trojanowski JQ: Consensus recommendations for the postmortem diagnosis of Alzheimer disease from the National Institute on Aging and the Reagan Institute Working Group on diagnostic criteria for the neuropathological assessment of Alzheimer disease. *J Neuropathol Exp Neurol* 1997, 56:1095–1097
16. Hammer A, Kager G, Dohr G, Rabl H, Ghassempur I, Jurgens G: Generation, characterization, and histochemical application of monoclonal antibodies selectively recognizing oxidatively modified apoB-containing serum lipoproteins. *Arterio Throm Vasc Biol* 1995, 15:704–713
17. Picklo MJ, Olson SJ, Markesbery WR, Montine TJ: Expression and activities of aldo-keto oxidoreductases in Alzheimer's disease. *J Neuropathol Exp Neurol* 2001, 60:686–695
18. Montine KS, Reich E, Olson SJ, Markesbery WR, Montine T: Distribution of reducible 4-hydroxynonenal adduct immunoreactivity in Alzheimer's disease is associated with APOE genotype. *J Neuropathol Exp Neurol* 1998, 57:415–425
19. Teupser D, Thiery J, Walli A, Seidel D: Determination of LDL- and scavenger-receptor activity in adherent and non-adherent cultured cells with a new single-step fluorometric assay. *Biochim Biophys Acta* 1996, 1303:193–198
20. Montine TJ, Beal MF, Cudkovicz ME, Brown RH, O'Donnell H, Margolin RA, McFarland L, Bachrach AF, Zackert WE, Roberts LJ, Morrow JD: Increased cerebrospinal fluid F<sub>2</sub>-isoprostane concentration in probable Alzheimer's disease. *Neurology* 1999, 52:562–565
21. Fessel JP, Porter NA, Moore KP, Sheller JR, Roberts LJ: Discovery of lipid peroxidation products formed in vivo with a substituted tetrahydrofuran ring (isofurans) that are favored by increased oxygen tension. *Proc Natl Acad Sci USA* 2002, 99:16713–16718
22. Ye Z, Sontheimer H: Metabotropic glutamate receptor agonists reduce glutamate release from cultured astrocytes. *Glia* 1999, 25:270–281
23. Montine T, Neely M, Quinn J, Beal M, Markesbery W, Roberts L, Morrow J: Lipid peroxidation in aging brain and Alzheimer's disease. *Free Radic Biol Med* 2002, 33:620–626
24. Imai H, Graham DJ, Masayasu H, Macrae IM: Antioxidant ebselen reduces oxidative damage in focal cerebral ischemia. *Free Radic Biol Med* 2002, 34:56–63
25. Neuzil J, Christison JK, Iheanacho E, Franonias JC, Zammit V, Hunt NH, Stocker R: Radical-induced lipoprotein and plasma lipid oxidation in normal and apolipoprotein E gene knockout (apoE  $-/-$ ) mice: apoE  $-/-$  mice as a model for testing the role of alpha-tocopherol-mediated peroxidation in atherogenesis. *J Lipid Res* 1998, 39:354–368
26. Esterbauer H, Dieber-Rotheneder M, Waeg G, Striegl G, Jurgens G: Biochemical, structural, and functional properties of oxidized low-density lipoprotein. *Chem Res Toxicol* 1990, 3:77–92
27. Lynch SM, Morrow JD, Roberts II LJ, Frei B: Formation of non-cyclooxygenase-derived prostanoids (F<sub>2</sub>-isoprostanes) in plasma and low density lipoprotein exposed to oxidative stress in vitro. *J Clin Invest* 1994, 93:998–1004
28. Plutzky J: Inflammatory pathways in atherosclerosis and acute coronary syndromes. *Am J Cardiol* 2001, 88:10K–15K
29. Dong Y, Benveniste EN: Immune function of astrocytes. *Glia* 2001, 36:180–190
30. Neumann-Haefelin T, Kastrup A, de Crespigny A, Yenari M, Ringer T, Sun G, Moseley M: Serial MRI after transient focal cerebral ischemia in rats: dynamics of tissue injury, blood-brain barrier damage, and edema formation. *Stroke* 2000, 31:1965–1972
31. Lerouet D, Beray-Berthet V, Palmier B, Plotkine M, Margail I: Changes in oxidative stress, iNOS activity and neutrophil infiltration in severe transient focal cerebral ischemia in rats. *Brain Res* 2002, 958:166–175
32. Vila N, Castillo J, Davalos A, Chamorro A: Proinflammatory cytokines and early neurological worsening in ischemic stroke. *Stroke* 2000, 31:2325–2329
33. Tarkowski E, Rosengren L, Blomstrand C, Wikkelso C, Jensen C, Ekholm S, Tarkowski A: Early intrathecal production of interleukin-6 predicts the size of brain lesion in stroke. *Stroke* 1995, 26:1393–1398
34. Clark WM, Beamer NB, Wynn M, Coull BM: The initial acute phase response predicts long-term stroke recovery. *J Stroke Cerebrovasc Dis* 1998, 7:128–131
35. Wang X, Yue TL, Young PR, Barone FC, Feuerstein GZ: Expression of interleukin-6, c-fos, and zif268 mRNAs in rat ischemic cortex. *J Cerebral Blood Flow Metab* 1995, 15:166–171
36. Clark WM, Rinker LG, Lessov NS, Hazel K, Hill JK, Stenzel-Poore M, Eckenstein F: Lack of interleukin-6 expression is not protective against focal central nervous system ischemia. *Stroke* 2000, 31:1715–1720
37. Massy ZA, Kim Y, Gujjarro C, Kasiske BL, Keane WF, O'Donnell MP: Low-density lipoprotein-induced expression of interleukin-6, a marker of human mesangial cell inflammation: effects of oxidation and modulation by lovastatin. *Biochem Biophys Res Commun* 2000, 267:536–540